

Supplementary Materials for “A Ready To Use Web-Application Providing a Personalized Biopsy Schedule for Men With Low-Risk PCa Under Active Surveillance”

Anirudh Tomer, MSc^{a,*}, Daan Nieboer, MSc^b, Monique J. Roobol, PhD^c,
Anders Bjartell, MD, PhD^d, Ewout W. Steyerberg, PhD^{b,e}, Dimitris
Rizopoulos, PhD^a, Movember Foundations Global Action Plan Prostate
Cancer Active Surveillance (GAP3) consortium^f

^a*Department of Biostatistics, Erasmus University Medical Center, Rotterdam, the
Netherlands*

^b*Department of Public Health, Erasmus University Medical Center, Rotterdam, the
Netherlands*

^c*Department of Urology, Erasmus University Medical Center, Rotterdam, the Netherlands*

^d*Department of Urology, Skåne University Hospital, Malmö, Sweden*

^e*Department of Biomedical Data Sciences, Leiden University Medical Center, Leiden, the
Netherlands*

^f*The Movember Foundations Global Action Plan Prostate Cancer Active Surveillance
(GAP3) consortium members presented in Appendix F*

1 **Appendix A. A Joint Model for the Longitudinal PSA, and Time** 2 **to Gleason Reclassification**

3 Let T_i^* denote the true time of reclassification (increase in biopsy Gleason
4 grade from 1 to 2 or higher) for the i -th patient included in PRIAS. Since
5 biopsies are conducted periodically, T_i^* is observed with interval censoring
6 $l_i < T_i^* \leq r_i$. When reclassification is observed for the patient at his latest

*Corresponding author (Anirudh Tomer): Erasmus MC, kamer flex Na-2823, PO Box
2040, 3000 CA Rotterdam, the Netherlands. Tel: +31 10 70 43393

Email addresses: a.tomer@erasmusmc.nl (Anirudh Tomer, MSc),
d.nieboer@erasmusmc.nl (Daan Nieboer, MSc), m.roobol@erasmusmc.nl (Monique J.
Roobol, PhD), anders.bjartell@med.lu.se (Anders Bjartell, MD, PhD),
e.w.steyerberg@lumc.nl (Ewout W. Steyerberg, PhD), d.rizopoulos@erasmusmc.nl
(Dimitris Rizopoulos, PhD)

7 biopsy time r_i , then l_i denotes the time of the second latest biopsy. Oth-
 8 erwise, l_i denotes the time of the latest biopsy and $r_i = \infty$. Let \mathbf{y}_i denote
 9 his observed PSA longitudinal measurements. The observed data of all n
 10 patients is denoted by $\mathcal{D}_n = \{l_i, r_i, \mathbf{y}_i; i = 1, \dots, n\}$.

In our joint model, the patient-specific PSA measurements over time are modeled using a linear mixed effects sub-model. It is given by (see Panel A, Figure 1):

$$\begin{aligned} \log_2 \{y_i(t) + 1\} &= m_i(t) + \varepsilon_i(t), \\ m_i(t) &= \beta_0 + b_{0i} + \sum_{k=1}^4 (\beta_k + b_{ki}) B_k\left(\frac{t-2}{2}, \frac{\mathcal{K}-2}{2}\right) + \beta_5 \text{age}_i, \end{aligned} \quad (1)$$

11 where, $m_i(t)$ denotes the measurement error free value of $\log_2(\text{PSA} + 1)$
 12 transformed $[2, 3]$ measurements at time t . We model it non-linearly over
 13 time using B-splines [4]. To this end, our B-spline basis function $B_k\{(t -$
 14 $2)/2, (\mathcal{K} - 2)/2\}$ has 3 internal knots at $\mathcal{K} = \{0.5, 1.3, 3\}$ years, which are
 15 the three quartiles of the observed follow-up times. The boundary knots of
 16 the spline are at 0 and 6.3 years (95-th percentile of the observed follow-
 17 up times). We mean centered (mean 2 years) and standardized (standard
 18 deviation 2 years) the follow-up time t and the knots of the B-spline \mathcal{K} during
 19 parameter estimation for better convergence. The fixed effect parameters are
 20 denoted by $\{\beta_0, \dots, \beta_5\}$, and $\{b_{0i}, \dots, b_{4i}\}$ are the patient specific random
 21 effects. The random effects follow a multivariate normal distribution with
 22 mean zero and variance-covariance matrix \mathbf{D} . The error $\varepsilon_i(t)$ is assumed to
 23 be t-distributed with three degrees of freedom (see Appendix B.1) and scale
 24 σ , and is independent of the random effects.

To model the impact of PSA measurements on the risk of reclassification, our joint model uses a relative risk sub-model. More specifically, the hazard of reclassification denoted as $h_i(t)$, and the cumulative risk of reclassification denoted as $R_i(t)$, at a time t are (see Panel C, Figure 1):

$$\begin{aligned} h_i(t) &= h_0(t) \exp \left(\gamma \text{age}_i + \alpha_1 m_i(t) + \alpha_2 \frac{dm_i(t)}{dt} \right), \\ R_i(t) &= \exp \left\{ - \int_0^t h_i(s) ds \right\}, \end{aligned} \quad (2)$$

where, γ is the parameter for the effect of age. The impact of PSA on the hazard of reclassification is modeled in two ways, namely the impact of

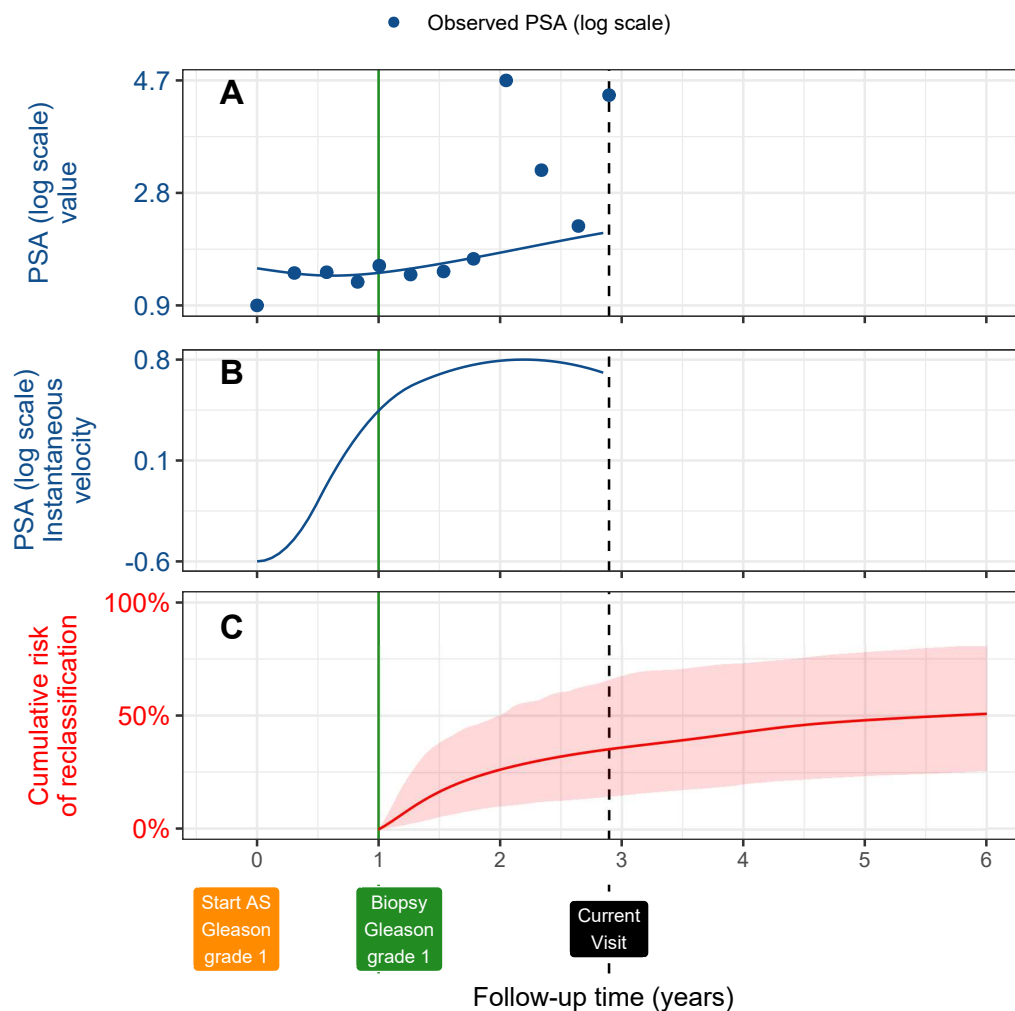


Figure 1: **Illustration of the joint model on a real PRIAS dataset patient.** **Panel A:** Observed (blue dots) and fitted PSA (solid blue line) measurements, log-transformed. **Panel B:** Estimated instantaneous velocity of PSA (log-transformed). **Panel C:** Predicted cumulative-risk of reclassification (95% credible interval shaded). Reclassification is defined as increase in Gleason grade [1] from grade 1 to 2 or higher. This risk of reclassification is available starting from the time of the latest negative biopsy (vertical green line at year 1 of follow-up). Joint model estimated it by combining the fitted PSA value and velocity (both on log scale of PSA) and time of latest negative biopsy. Black dashed line at year 4 denotes time of current visit.

the error free underlying PSA value $m_i(t)$ (see Panel A, Figure 1), and the impact of the underlying PSA velocity $dm_i(t)/dt$ (see Panel B, Figure 1). The corresponding parameters are α_1 and α_2 , respectively. Lastly, $h_0(t)$ is the baseline hazard at time t , and is modeled flexibly using P-splines [5]. More specifically:

$$\log h_0(t) = \gamma_{h_0,0} + \sum_{q=1}^Q \gamma_{h_0,q} B_q(t, \mathbf{v}),$$

where $B_q(t, \mathbf{v})$ denotes the q -th basis function of a B-spline with knots $\mathbf{v} = v_1, \dots, v_Q$ and vector of spline coefficients γ_{h_0} . To avoid choosing the number and position of knots in the spline, a relatively high number of knots (e.g., 15 to 20) are chosen and the corresponding B-spline regression coefficients γ_{h_0} are penalized using a differences penalty [5].

We estimate the parameters of the joint model using Markov chain Monte Carlo (MCMC) methods under the Bayesian framework. Let $\boldsymbol{\theta}$ denote the vector of all of the parameters of the joint model. The joint model postulates that given the random effects, the time of reclassification, and the PSA measurements taken over time are all mutually independent. Under this assumption the posterior distribution of the parameters is given by:

$$\begin{aligned} p(\boldsymbol{\theta}, \mathbf{b} \mid \mathcal{D}_n) &\propto \prod_{i=1}^n p(l_i, r_i, \mathbf{y}_i \mid \mathbf{b}_i, \boldsymbol{\theta}) p(\mathbf{b}_i \mid \boldsymbol{\theta}) p(\boldsymbol{\theta}) \\ &\propto \prod_{i=1}^n p(l_i, r_i \mid \mathbf{b}_i, \boldsymbol{\theta}) p(\mathbf{y}_i \mid \mathbf{b}_i, \boldsymbol{\theta}) p(\mathbf{b}_i \mid \boldsymbol{\theta}) p(\boldsymbol{\theta}), \\ p(\mathbf{b}_i \mid \boldsymbol{\theta}) &= \frac{1}{\sqrt{(2\pi)^q \det(\mathbf{D})}} \exp \left\{ -\frac{1}{2} (\mathbf{b}_i^T \mathbf{D}^{-1} \mathbf{b}_i) \right\}, \end{aligned}$$

where, the likelihood contribution of the PSA outcome, conditional on the random effects is:

$$p(\mathbf{y}_i \mid \mathbf{b}_i, \boldsymbol{\theta}) = \frac{1}{(\sqrt{2\pi}\sigma^2)^{n_i}} \exp \left\{ -\frac{\sum_{j=1}^{n_i} (y_{ij} - m_{ij})^2}{2\sigma^2} \right\},$$

where n_i is the number of PSA measurements of the i -th patient. The likelihood contribution of the time of reclassification outcome is given by:

$$p(l_i, r_i \mid \mathbf{b}_i, \boldsymbol{\theta}) = \exp \left\{ -\int_0^{l_i} h_i(s) ds \right\} - \exp \left\{ -\int_0^{r_i} h_i(s) ds \right\}. \quad (3)$$

30 The integrals in (3) do not have a closed-form solution, and therefore we use
 31 a 15-point Gauss-Kronrod quadrature rule to approximate them.

32 We use independent normal priors with zero mean and variance 100 for
 33 the fixed effects $\{\beta_0, \dots, \beta_5\}$, and inverse Gamma prior with shape and rate
 34 both equal to 0.01 for the parameter σ^2 . For the variance-covariance matrix
 35 \mathbf{D} of the random effects we take inverse Wishart prior with an identity scale
 36 matrix and degrees of freedom equal to 5 (number of random effects). For
 37 the relative risk model's parameter γ and the association parameters α_1, α_2 ,
 38 we use independent normal priors with zero mean and variance 100.

39 *Appendix A.1. Assumption of t-distributed (df=3) Error Terms*

40 With regards to the choice of the distribution for the error term ε for
 41 the PSA measurements (see Equation 1), we attempted fitting multiple joint
 42 models differing in error distribution, namely t-distribution with three, and
 43 four degrees of freedom, and a normal distribution for the error term. How-
 44 ever, the model assumption for the error term were best met by the model
 45 with t-distribution having three degrees of freedom. The quantile-quantile
 46 plot of subject-specific residuals for the corresponding model in Panel A of
 47 Figure 2, shows that the assumption of t-distributed (df=3) errors is reason-
 48 ably met by the fitted model.

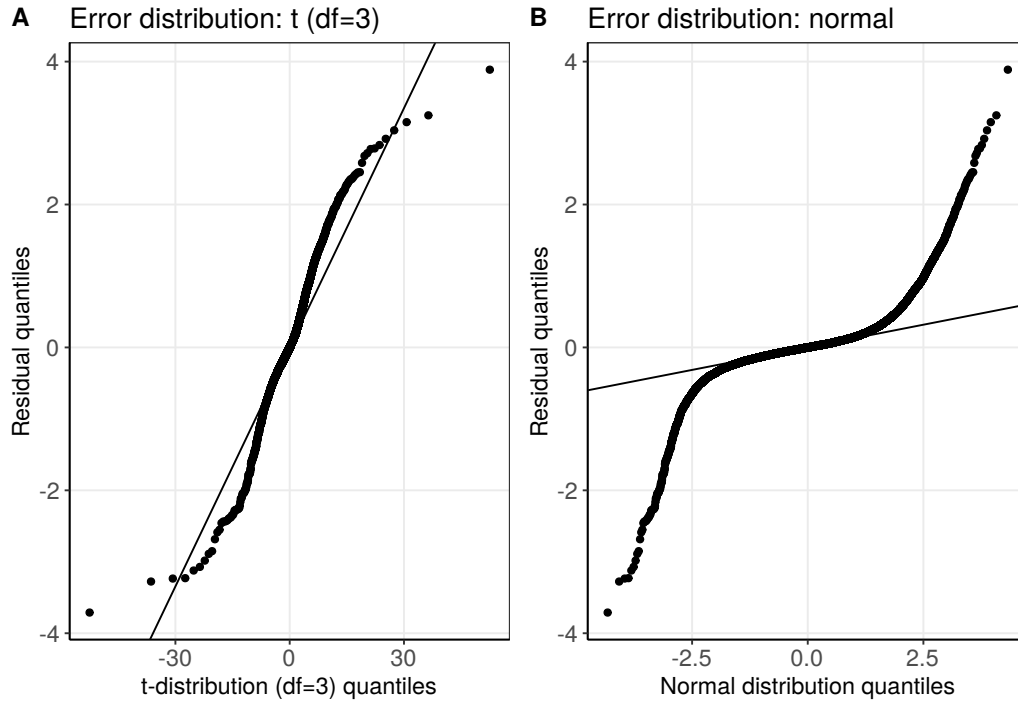


Figure 2: **Quantile-quantile plot** of subject-specific PSA residuals from two different joint models fitted to the PRIAS dataset. **Panel A:** model assuming a t-distribution ($df=3$) for the error term ε (see Equation 1). **Panel B:** model assuming a normal distribution for the error term ε .

Table 1: **Estimated variance-covariance matrix D** of the random effects $\mathbf{b} = (b_0, b_1, b_2, b_3, b_4)$ from the joint model fitted to the PRIAS dataset. The variances of the random effects are highlighted along the diagonal of the variance-covariance matrix.

Random Effects	b_0	b_1	b_2	b_3	b_4
b_0	0.229	0.030	0.023	0.073	0.007
b_1	0.030	0.149	0.098	0.171	0.085
b_2	0.023	0.098	0.276	0.335	0.236
b_3	0.073	0.171	0.335	0.560	0.359
b_4	0.007	0.085	0.236	0.359	0.351

Table 2: **Parameters of the longitudinal sub-model:** Estimated mean and 95% credible interval for parameters in Equation (1).

Variable	Mean	Std. Dev	2.5%	97.5%	P
Intercept	2.129	0.060	2.009	2.244	<0.001
Age	0.008	0.001	0.007	0.010	<0.001
Spline: [0.0, 0.5] years	0.063	0.007	0.051	0.075	<0.001
Spline: [0.5, 1.3] years	0.196	0.010	0.177	0.217	<0.001
Spline: [1.3, 3.0] years	0.244	0.014	0.217	0.272	<0.001
Spline: [3.0, 6.3] years	0.382	0.014	0.356	0.410	<0.001
σ	0.139	0.001	0.138	0.140	

49 Appendix A.2. Results

50 The joint model was fitted using the R package **JMbayes** [8]. This pack-
 51 age utilizes the Bayesian methodology to estimate model parameters. The
 52 corresponding posterior parameter estimates are shown in Table 2 (longitu-
 53 dinal sub-model for PSA outcome) and Table 3 (relative risk sub-model).
 54 The parameter estimates for the variance-covariance matrix D from the lon-
 55 gitudinal sub-model for PSA are shown in the following Table 1:

56 For the PSA mixed effects sub-model parameter estimates (see Equa-
 57 tion 1), in Table 2 we can see that the age of the patient trivially affects
 58 the baseline $\log_2(\text{PSA} + 1)$ measurement. Since the longitudinal evolution of
 59 $\log_2(\text{PSA} + 1)$ measurements is modeled with non-linear terms, the interpre-
 60 tation of the coefficients corresponding to time is not straightforward. In lieu
 61 of the interpretation, in Figure 4 we present plots of observed versus fitted
 62 PSA profiles for nine randomly selected patients.

63 For the relative risk sub-model (see Equation 2), the parameter estimates
 64 in Table 3 show that $\log_2(\text{PSA} + 1)$ velocity and age of the patient were
 65 significantly associated with the hazard of reclassification.

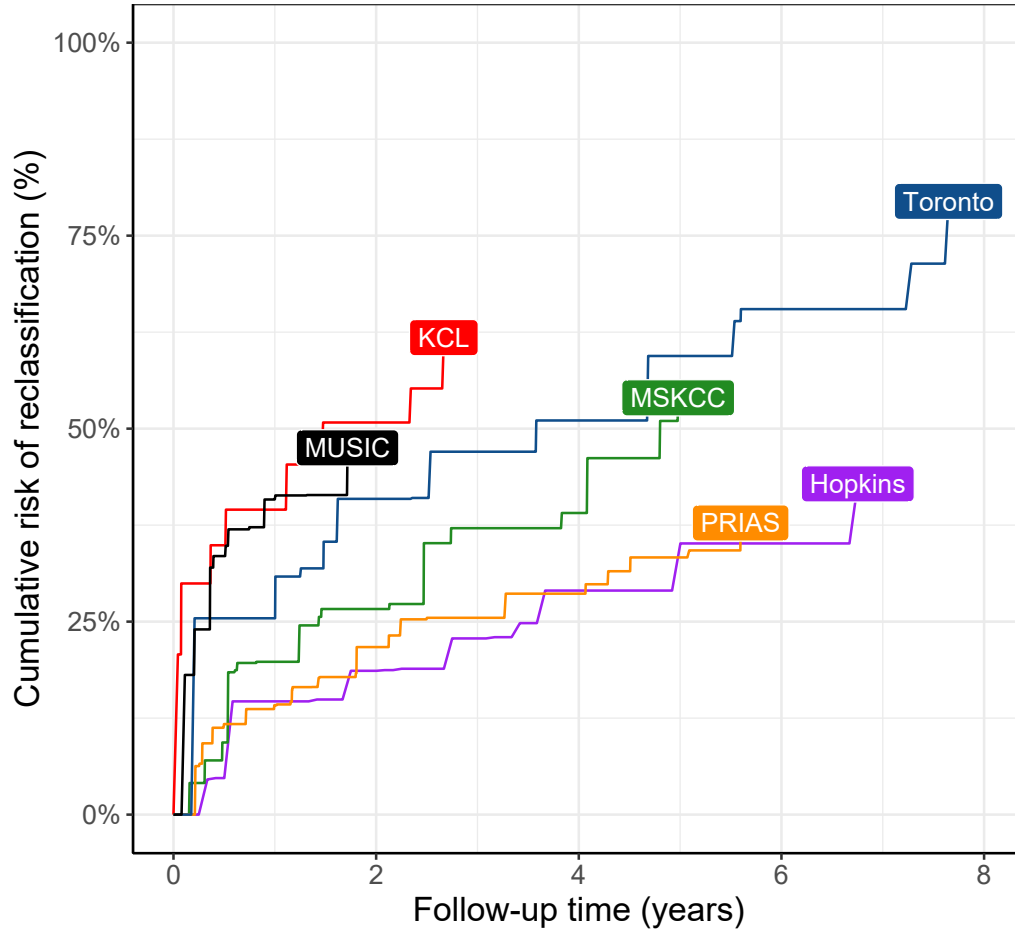


Figure 3: **Nonparametric estimate [6] of cumulative risk of reclassification** in the world's largest AS cohort PRIAS, and largest five AS cohorts from the GAP3 database [7]. Abbreviations are *Hopkins*: Johns Hopkins Active Surveillance, *PRIAS*: Prostate Cancer International Active Surveillance, *Toronto*: University of Toronto Active Surveillance, *MSKCC*: Memorial Sloan Kettering Cancer Center Active Surveillance, *KCL*: King's College London Active Surveillance, *MUSIC*: Michigan Urological Surgery Improvement Collaborative AS.

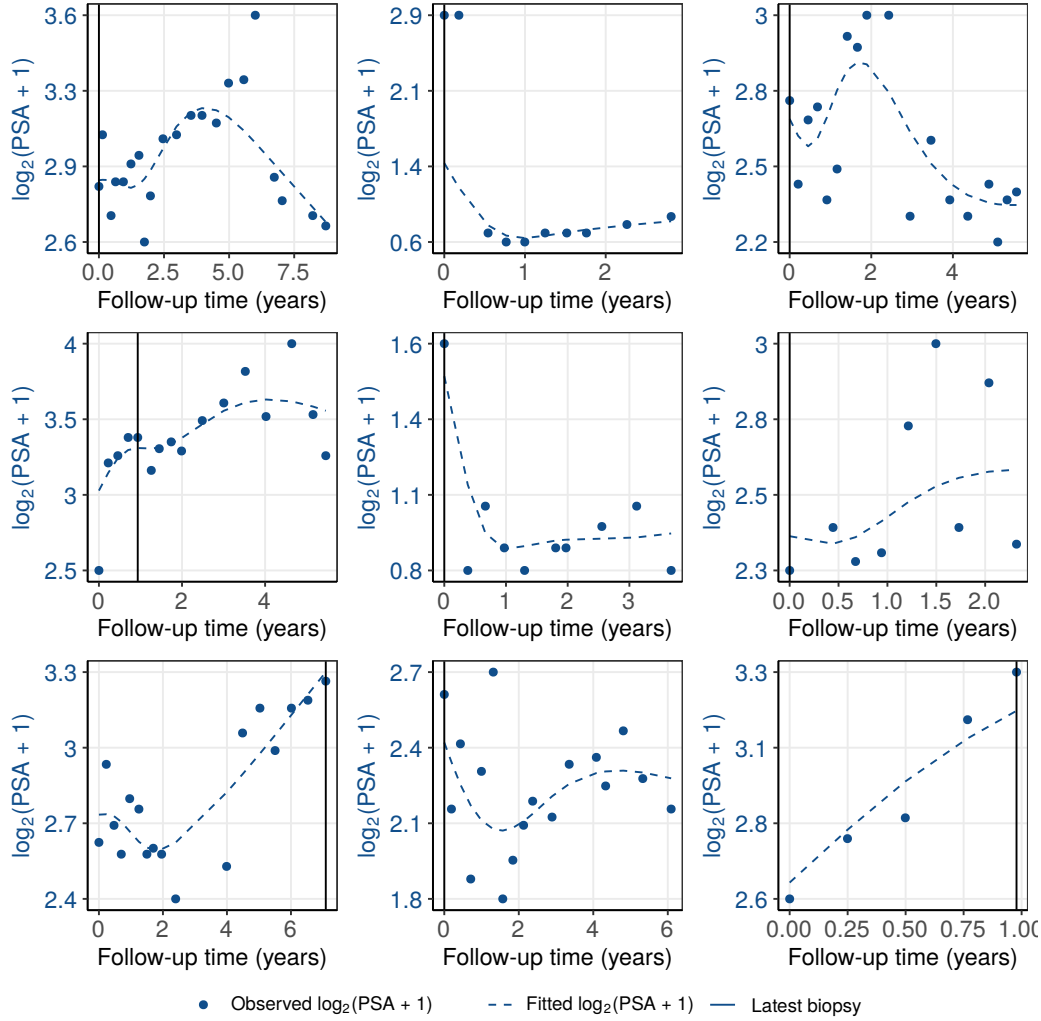


Figure 4: **Fitted versus observed $\log_2(\text{PSA} + 1)$ profiles** for nine randomly selected PRIAS patients. The fitted profiles utilize information from the observed PSA measurements, and time of the latest biopsy.

Table 3: **Parameters of the relative risk sub-model:** Estimated mean and 95% credible interval for the parameters in Equation (2).

Variable	Mean	Std. Dev	2.5%	97.5%	P
Age	0.037	0.006	0.025	0.049	<0.001
Fitted $\log_2(\text{PSA} + 1)$ value	-0.012	0.076	-0.164	0.135	0.856
Fitted $\log_2(\text{PSA} + 1)$ velocity	2.266	0.299	1.613	2.767	<0.001

Table 4: **Hazard ratio and 95% credible interval (CI) for reclassification:** Variables are on different scale and hence we compare an increase in the variables of relative risk sub-model from their 25-th percentile (P_{25}) to their 75-th percentile (P_{75}). Except for age, quartiles for all other variables are based on their fitted values obtained from the joint model fitted to the PRIAS dataset.

Variable	P_{25}	P_{75}	Hazard ratio [95% CI]
Age	61	71	1.455 [1.285, 1.631]
Fitted $\log_2(\text{PSA} + 1)$ value	2.360	3.078	0.991 [0.889, 1.102]
Fitted $\log_2(\text{PSA} + 1)$ velocity	-0.085	0.308	2.433 [1.883, 2.962]

It is important to note that since age, and $\log_2(\text{PSA} + 1)$ value and velocity are all measured on different scales, a comparison between the corresponding parameter estimates is not easy. To this end, in Table 4, we present the hazard ratio of reclassification, for an increase in the aforementioned variables from their 25-th to the 75-th percentile. For example, an increase in fitted $\log_2(\text{PSA} + 1)$ velocity from -0.085 to 0.308 (fitted 25-th and 75-th percentiles) corresponds to a hazard ratio of 2.433. The interpretation for the rest is similar.

74 Appendix B. Risk Predictions for Reclassification

Let us assume a new patient j , for whom we need to estimate the risk of reclassification. Let his current follow-up visit time be s , latest time of biopsy be t , observed vector PSA measurements be $\mathcal{Y}_j(s)$. The combined information from the observed data about the time of reclassification, is given by the following posterior predictive distribution $g(T_j^*)$ of his time T_j^* of reclassification:

$$\begin{aligned} g(T_j^*) &= p\{T_j^* \mid T_j^* > t, \mathcal{Y}_j(s), \mathcal{D}_n\} \\ &= \int \int p(T_j^* \mid T_j^* > t, \mathbf{b}_j, \boldsymbol{\theta}) \\ &\quad \times p\{\mathbf{b}_j \mid T_j^* > t, \mathcal{Y}_j(s), \boldsymbol{\theta}\} p(\boldsymbol{\theta} \mid \mathcal{D}_n) d\mathbf{b}_j d\boldsymbol{\theta}. \end{aligned}$$

75 The distribution $g(T_j^*)$ depends not only depends on the observed data of the
 76 patient $T_j^* > t, \mathcal{Y}_j(s)$, but also depends on the information from the PRIAS
 77 dataset \mathcal{D}_n . To this the the posterior distribution of random effects \mathbf{b}_j and
 78 posterior distribution of the vector of all parameters $\boldsymbol{\theta}$ are utilized, respec-
 79 tively. The distribution $g(T_j^*)$ can be estimated as detailed in Rizopoulos
 80 et al. [9]. Since, majority of the prostate cancer patients may not obtain
 81 reclassification in the current follow-up period of PRIAS (thirteen years),
 82 $g(T_j^*)$ can only be estimated for a currently limited follow-up period.

The cumulative risk of reclassification can be derived from $g(T_j^*)$ as given in [9]. It is given by:

$$R_j(u \mid t, s) = \Pr\{T_j^* > u \mid T_j^* > t, \mathcal{Y}_j(s), \mathcal{D}_n\}, \quad u \geq t. \quad (4)$$

83 The personalized risk profile of the patient (see Panel C, Figure 5) updates
 84 as more data is gathered over follow-up visits.

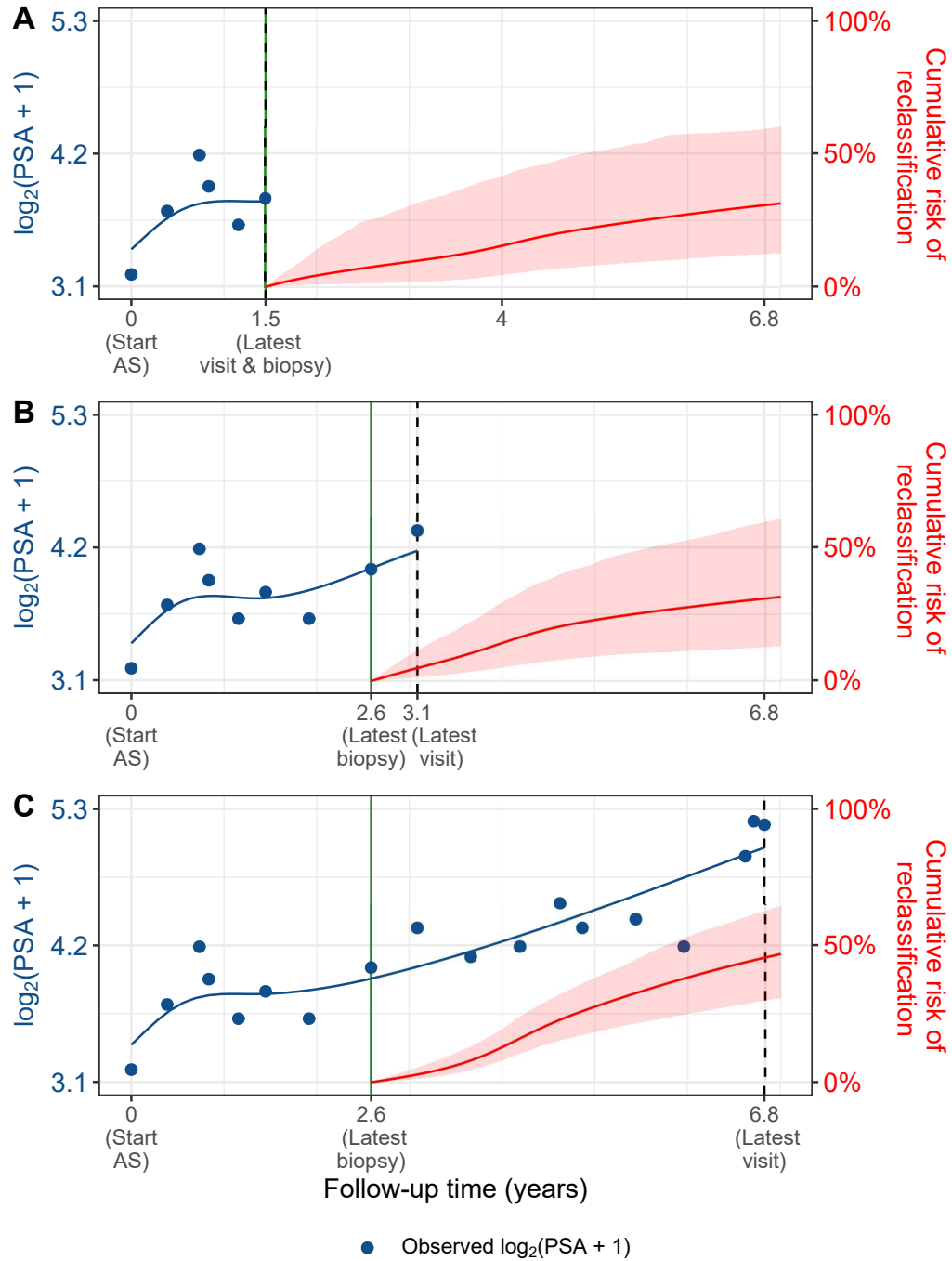


Figure 5: **Cumulative risk of (reclassification) changing dynamically over follow-up** as more patient data is gathered. The three **Panels A,B and C**: are ordered by the time of the latest visit (dashed vertical black line) of a new patient. At each of the latest follow-up visits, we combine the accumulated PSA measurements (shown in blue), and latest time of negative biopsy (solid vertical green line) to obtain the updated cumulative risk profile (shown in red) of the patient.

85 *Appendix B.1. Validation of Risk Predictions*

86 We wanted to check the usefulness of our model for not only the PRIAS
 87 patients but also for patients from other cohorts. To this end, we validated
 88 our model in the PRIAS dataset (internal validation) and in largest five co-
 89 horts from the GAP3 database [7]. These are the University of Toronto AS
 90 (Toronto), Johns Hopkins AS (Hopkins), Memorial Sloan Kettering Cancer
 91 Center AS (MSKCC), King’s College London AS (KCL), and Michigan Uro-
 92 logical Surgery Improvement Collaborative AS (MUSIC).

Calibration-in-the-large We first assessed calibration-in-the-large [10]
 of our model in the aforementioned cohorts. To this end, we used our model
 to predict the cumulative risk of reclassification for each patient given their
 PSA measurements and biopsy results. We then averaged the resulting pro-
 files of cumulative risk of reclassification. Subsequently we compared the
 averaged cumulative-risk profile with a non-parametric estimate [6] of the
 cumulative risk of reclassification in each of the cohorts. The results are
 shown in Panel A of Figure 6. We can see that our model’s calibration is fine
 only in PRIAS and Hopkins cohorts. To improve our model’s calibration in
 KCL, MUSIC, Toronto, and MSKCC cohorts, we recalibrated the baseline
 hazard of the joint model fitted to the PRIAS dataset, individually for each
 of these cohorts. More specifically, given the data of an external cohort \mathcal{D}_n^c ,
 where c denotes the cohort, the recalibrated parameters γ_{h0}^c (Appendix A)
 of the log baseline hazard are given by:

$$p(\gamma_{h0}^c \mid \mathcal{D}_n^c, \mathbf{b}^c, \boldsymbol{\theta}) \propto \prod_{i=1}^{n^c} p(l_i^c, r_i^c \mid \mathbf{b}_i^c, \boldsymbol{\theta}) p(\gamma_{h0}^c) \quad (5)$$

93 where n^c are the number of patients in the c -th cohort and $\boldsymbol{\theta}$ are the pa-
 94 rameters of the joint model fitted to the PRIAS dataset. The interval in
 95 which reclassification is observed for the i – th patient is given by l_i^c, r_i^c , with
 96 $r_i^c = \infty$ for right censored patients. The symbol \mathbf{b}_i^c denotes patient-specific
 97 random effects (Appendix A). The random effects are obtained using the joint
 98 model fitted to the PRIAS dataset prior to recalibration. We re-evaluated the
 99 calibration-in-the-large of our model after the recalibration of the baseline
 100 hazard individually for each cohort. The improved calibration-in-the-large is
 101 shown in Panel B of Figure 6.

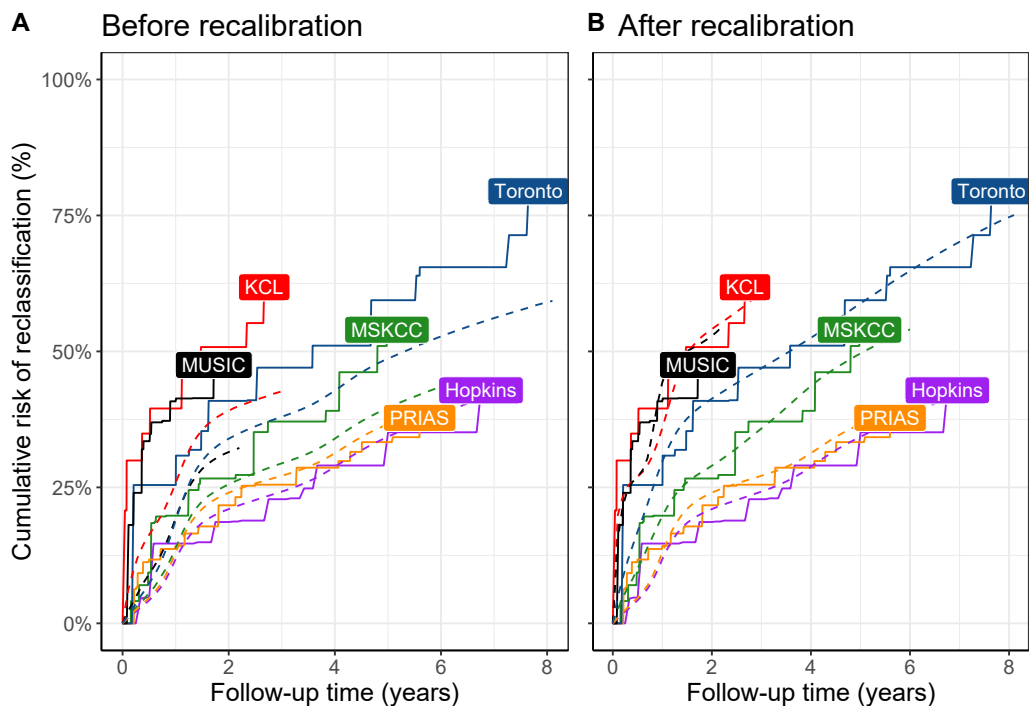


Figure 6: **Calibration-in-the-large of our model:** In **Panel A** we can see that our model is not well calibrated for use in KCL, MUSIC, Toronto and MSKCC. In **Panel B** we can see that calibration of model predictions improved in KCL, MUSIC, Toronto and MSKCC cohorts after recalibrating our model. Recalibration was not necessary for Hopkins cohort. Full names of Cohorts are *PRIAS*: Prostate Cancer International Active Surveillance, *Toronto*: University of Toronto Active Surveillance, *Hopkins*: Johns Hopkins Active Surveillance, *MSKCC*: Memorial Sloan Kettering Cancer Center Active Surveillance, *KCL*: King's College London Active Surveillance, *MUSIC*: Michigan Urological Surgery Improvement Collaborative Active Surveillance.

102 ***Recalibrated PRIAS Model Versus Individual Joint Models***
 103 ***For Each Cohort*** We wanted to check if our recalibrated PRIAS model
 104 performed as good as a new joint model that could be fitted to the external
 105 cohorts. To this end, we predicted cumulative-risk of reclassification for each
 106 patient from each cohort using two different models, namely the recalibrated
 107 PRIAS model for that cohort, and a new joint model fitted to that cohort.
 108 The difference in predicted cumulative-risk of reclassification from these co-
 109 horts (Figure 7) is quite small. The only exception is the MUSIC cohort
 110 in which individual risk predictions obtained from the recalibrated PRIAS
 111 model may differ from predictions from a newly fitted joint model, by more
 112 than 10% in at least half of the patients.

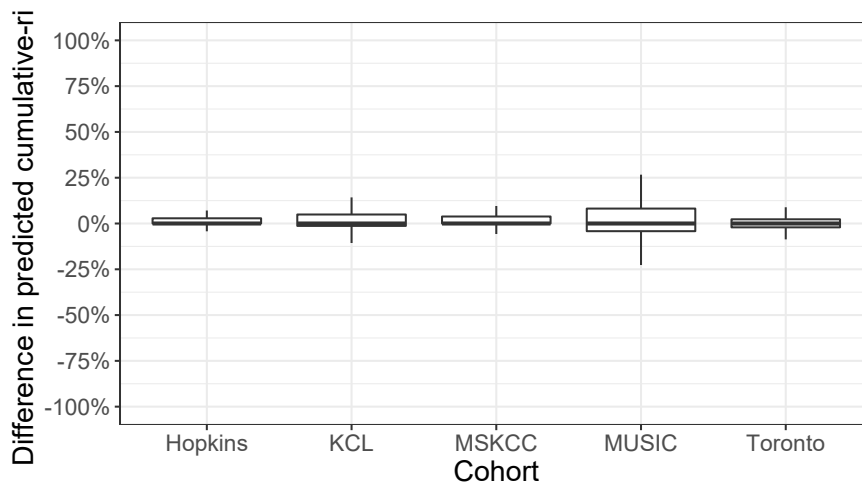


Figure 7: **Comparison of predictions from recalibrated PRIAS model with individual joint models fitted to external cohorts:** On Y-axis we show the difference between predicted cumulative-risk of reclassification for individual patients using two models, namely the recalibrated PRIAS model for each cohort, and individual joint model fitted to each cohort. The maximum differences in each direction can be 100% or -100%. The figure shows that in all cohorts except the MUSIC cohort, the recalibrated PRIAS model predicts as good as a newly fitted joint model to each of the cohorts. Full names of Cohorts are *PRIAS*: Prostate Cancer International Active Surveillance, *Toronto*: University of Toronto Active Surveillance, *Hopkins*: Johns Hopkins Active Surveillance, *MSKCC*: Memorial Sloan Kettering Cancer Center Active Surveillance, *KCL*: King's College London Active Surveillance, *MUSIC*: Michigan Urological Surgery Improvement Collaborative Active Surveillance.

Validation of Dynamic Cumulative-Risk Predictions As shown in Figure 5 the cumulative-risk predictions from the joint model are dynamic in nature. That is, they update as more data becomes available over time. Consequently, the discrimination and calibration of the joint model also depends on the available data. We assessed these two measures dynamically in the PRIAS cohort (interval validation) and in the largest five external cohorts that are part of the GAP3 database. For discrimination we utilized the time-varying area under the receiver operating characteristic curve or time-varying AUC [9]. For time-varying calibration we assessed the mean absolute prediction error or MAPE [9]. The AUC indicates how well the model discriminates between patients who experience reclassification and those do not. The MAPE indicates how accurately the model predicts reclassification. Both AUC and MAPE are restricted to $[0, 1]$. However, it is preferred that $\text{AUC} > 0.5$ because an $\text{AUC} \leq 0.5$ indicates that the model performs worse than random discrimination. Ideally MAPE should be 0.

We calculate AUC and MAPE in a time-dependent manner. More specifically, given the time of latest biopsy t , and history of PSA measurements up to time s , we calculate AUC and MAPE for a medically relevant time frame $(t, s]$, within which the occurrence of reclassification is of interest. In the case of prostate cancer, at any point in time s it is of interest to identify patients who may have experienced reclassification in the last one year $(s - 1, s]$. That is we set $t = s - 1$. We then calculate AUC and MAPE at a gap of every six months (follow-up schedule of PRIAS). That is, $s \in \{1, 1.5, \dots\}$ years. To obtain reliable estimates of AUC and MAPE, in each cohort we restrict s to a maximum time point s_{\max} , such that there are at least 10 patients who experience reclassification after s_{\max} . This maximum time point s_{\max} differs between cohorts, and is given in Table 5.

The results for estimates of AUC and MAPE are summarized in Figure 8, and in Table 6 to Table 11. Results are based on the recalibrated PRIAS model for Toronto, MSKCC, MUSIC, and KCL cohorts, whereas original joint model fitted to the PRIAS dataset is used for Hopkins and PRIAS cohorts. The results show that AUC remains more or less constant in all cohorts as more data becomes available for patients. The AUC obtains a moderate value, roughly between 0.5 and 0.7 for all cohorts. On the other hand, MAPE reduces by a big margin after year two of follow-up. This could be because of two reasons. Firstly, MAPE at year one is based only on four PSA measurements gathered in first year of follow-up, whereas after year two number of PSA measurements increase. Secondly, patients in year one consist

Table 5: **Maximum follow-up period up to which we can reliably predict risk of reclassification.** In each cohort, this time point is chosen such that there are at least 10 patients who experience reclassification after this time point. Full names of Cohorts are *PRIAS*: Prostate Cancer International Active Surveillance, *Toronto*: University of Toronto Active Surveillance, *Hopkins*: Johns Hopkins Active Surveillance, *MSKCC*: Memorial Sloan Kettering Cancer Center Active Surveillance, *KCL*: King's College London Active Surveillance, *MUSIC*: Michigan Urological Surgery Improvement Collaborative Active Surveillance.

Cohort	Maximum Prediction Time (years)
PRIAS	6
KCL	3
MUSIC	2
Toronto	8
MSKCC	6
Hopkins	7

151 of two sub-populations, namely patients with a correct Gleason grade 1 at the
 152 time of inclusion in AS, and patients who probably had Gleason grade 2 at
 153 inclusion but were misclassified by the urologist as Gleason grade 1 patients.
 154 To remedy this problem, a biopsy for all patients at year one is commonly
 155 recommended in all AS programs [11].

Table 6: **Internal validation of predictions of reclassification in PRIAS cohort.** The area under the receiver operating characteristic curve or AUC (measure of discrimination) and mean absolute prediction error or MAPE (measure of calibration) are calculated over the follow-up period at a gap of 6 months. In addition bootstrapped 95% confidence intervals (CI) are also presented.

Follow-up period (years)	AUC (95% CI)	MAPE (95%CI)
0.0 to 1.0	0.652 [0.611, 0.690]	0.220 [0.214, 0.227]
0.5 to 1.5	0.657 [0.641, 0.673]	0.260 [0.254, 0.265]
1.0 to 2.0	0.661 [0.647, 0.678]	0.187 [0.183, 0.191]
1.5 to 2.5	0.647 [0.596, 0.688]	0.129 [0.122, 0.140]
2.0 to 3.0	0.683 [0.642, 0.723]	0.135 [0.125, 0.146]
2.5 to 3.5	0.692 [0.632, 0.748]	0.118 [0.111, 0.128]
3.0 to 4.0	0.657 [0.603, 0.709]	0.086 [0.080, 0.092]
3.5 to 4.5	0.623 [0.582, 0.660]	0.111 [0.105, 0.116]
4.0 to 5.0	0.619 [0.582, 0.654]	0.126 [0.118, 0.131]
4.5 to 5.5	0.624 [0.537, 0.711]	0.119 [0.103, 0.135]
5.0 to 6.0	0.639 [0.582, 0.696]	0.121 [0.103, 0.138]

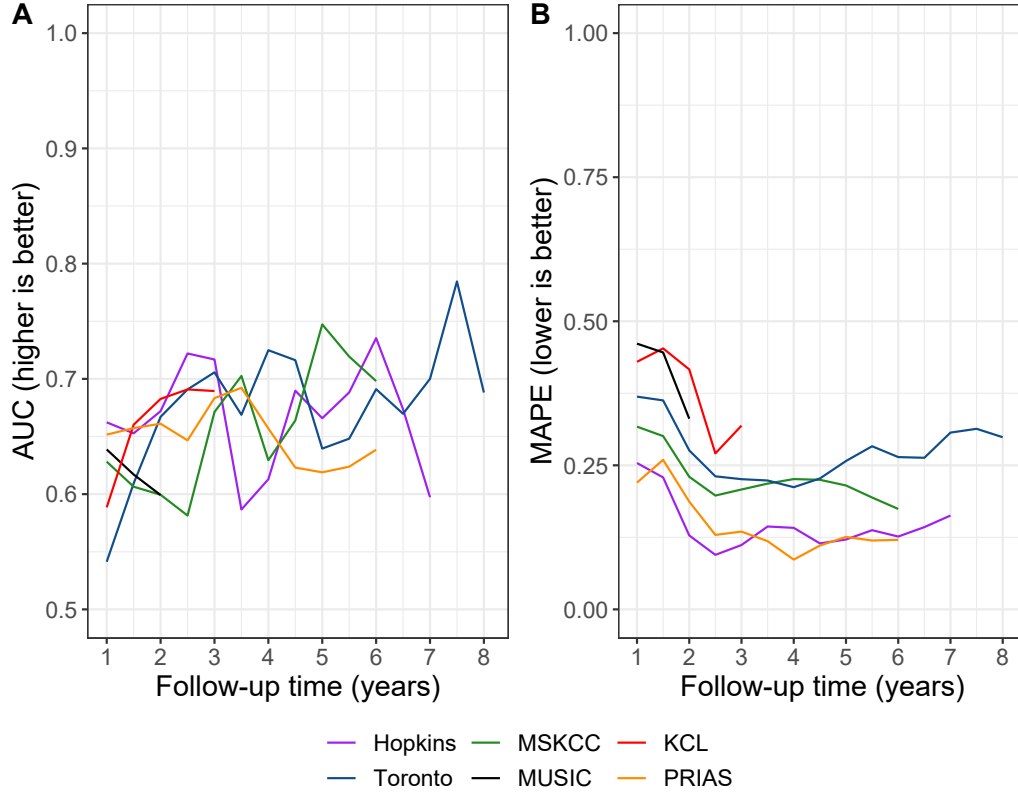


Figure 8: **Validation of Dynamic Cumulative-Risk Predictions.** In **Panel A** we can see that the time dependent area under the receiver operating characteristic curve or AUC (measure of discrimination) is above 0.5 in PRIAS (internal validation), and in Toronto, Hopkins, MSKCC, KCL, and MUSIC AS cohorts (external validation). In **Panel B** we can see that the time dependent root mean squared prediction error or MAPE (measure of calibration) is similar for PRIAS, and Hopkins and Toronto cohorts. The bootstrapped 95% confidence interval for these estimates are presented in Table 6 to Table 10. Full names of Cohorts are *PRIAS*: Prostate Cancer International Active Surveillance, *Toronto*: University of Toronto Active Surveillance, *Hopkins*: Johns Hopkins Active Surveillance, *MSKCC*: Memorial Sloan Kettering Cancer Center Active Surveillance, *KCL*: King's College London Active Surveillance, *MUSIC*: Michigan Urological Surgery Improvement Collaborative Active Surveillance.

Table 7: **External validation of predictions of reclassification in University of Toronto Active Surveillance cohort.** The area under the receiver operating characteristic curve or AUC (measure of discrimination) and mean absolute prediction error or MAPE (measure of calibration) are calculated over the follow-up period at a gap of 6 months. In addition bootstrapped 95% confidence intervals (CI) are also presented.

Follow-up period (years)	AUC (95% CI)	MAPE (95%CI)
0.0 to 1.0	0.541 [0.470, 0.621]	0.369 [0.352, 0.381]
0.5 to 1.5	0.609 [0.547, 0.661]	0.363 [0.348, 0.376]
1.0 to 2.0	0.667 [0.634, 0.712]	0.276 [0.259, 0.296]
1.5 to 2.5	0.691 [0.651, 0.730]	0.231 [0.205, 0.254]
2.0 to 3.0	0.706 [0.637, 0.762]	0.226 [0.196, 0.260]
2.5 to 3.5	0.669 [0.586, 0.741]	0.224 [0.195, 0.258]
3.0 to 4.0	0.725 [0.649, 0.806]	0.212 [0.184, 0.238]
3.5 to 4.5	0.716 [0.642, 0.793]	0.227 [0.206, 0.258]
4.0 to 5.0	0.640 [0.579, 0.717]	0.257 [0.222, 0.312]
4.5 to 5.5	0.648 [0.579, 0.740]	0.283 [0.247, 0.326]
5.0 to 6.0	0.691 [0.608, 0.793]	0.264 [0.232, 0.302]
5.5 to 6.5	0.670 [0.543, 0.776]	0.263 [0.227, 0.307]
6.0 to 7.0	0.700 [0.544, 0.851]	0.307 [0.258, 0.363]
6.5 to 7.5	0.785 [0.640, 0.866]	0.313 [0.272, 0.360]
7.0 to 8.0	0.688 [0.532, 0.786]	0.299 [0.249, 0.361]

Table 8: **External validation of predictions of reclassification in Johns Hopkins Active Surveillance cohort.** The area under the receiver operating characteristic curve or AUC (measure of discrimination) and mean absolute prediction error or MAPE (measure of calibration) are calculated over the follow-up period at a gap of 6 months. In addition bootstrapped 95% confidence intervals (CI) are also presented.

Follow-up period (years)	AUC (95% CI)	MAPE (95%CI)
0.0 to 1.0	0.662 [0.586, 0.715]	0.254 [0.245, 0.265]
0.5 to 1.5	0.653 [0.603, 0.707]	0.229 [0.219, 0.240]
1.0 to 2.0	0.672 [0.604, 0.744]	0.128 [0.115, 0.141]
1.5 to 2.5	0.722 [0.652, 0.792]	0.095 [0.081, 0.111]
2.0 to 3.0	0.717 [0.638, 0.777]	0.112 [0.100, 0.123]
2.5 to 3.5	0.587 [0.493, 0.704]	0.144 [0.129, 0.154]
3.0 to 4.0	0.613 [0.486, 0.742]	0.141 [0.126, 0.156]
3.5 to 4.5	0.690 [0.594, 0.783]	0.115 [0.100, 0.133]
4.0 to 5.0	0.666 [0.572, 0.754]	0.121 [0.104, 0.147]
4.5 to 5.5	0.688 [0.519, 0.779]	0.137 [0.119, 0.161]
5.0 to 6.0	0.735 [0.676, 0.820]	0.126 [0.102, 0.152]
5.5 to 6.5	0.674 [0.581, 0.765]	0.143 [0.121, 0.172]
6.0 to 7.0	0.597 [0.472, 0.712]	0.163 [0.126, 0.195]

Table 9: **External validation of predictions of reclassification in Memorial Sloan Kettering Cancer Center Active Surveillance cohort.** The area under the receiver operating characteristic curve or AUC (measure of discrimination) and mean absolute prediction error or MAPE (measure of calibration) are calculated over the follow-up period at a gap of 6 months. In addition bootstrapped 95% confidence intervals (CI) are also presented.

Follow-up period (years)	AUC (95% CI)	MAPE (95%CI)
0.0 to 1.0	0.628 [0.577, 0.688]	0.317 [0.316, 0.318]
0.5 to 1.5	0.606 [0.532, 0.657]	0.301 [0.290, 0.311]
1.0 to 2.0	0.599 [0.518, 0.671]	0.230 [0.207, 0.256]
1.5 to 2.5	0.581 [0.504, 0.663]	0.198 [0.168, 0.235]
2.0 to 3.0	0.671 [0.599, 0.741]	0.208 [0.182, 0.232]
2.5 to 3.5	0.703 [0.610, 0.777]	0.218 [0.197, 0.246]
3.0 to 4.0	0.629 [0.499, 0.706]	0.226 [0.194, 0.259]
3.5 to 4.5	0.664 [0.589, 0.756]	0.225 [0.199, 0.262]
4.0 to 5.0	0.747 [0.642, 0.841]	0.215 [0.188, 0.247]
4.5 to 5.5	0.719 [0.597, 0.852]	0.194 [0.165, 0.232]
5.0 to 6.0	0.698 [0.565, 0.792]	0.174 [0.136, 0.227]

Table 10: **External validation of predictions of reclassification in King's College London Active Surveillance cohort.** The area under the receiver operating characteristic curve or AUC (measure of discrimination) and mean absolute prediction error or MAPE (measure of calibration) are calculated over the follow-up period at a gap of 6 months. In addition bootstrapped 95% confidence intervals (CI) are also presented.

Follow-up period (years)	AUC (95% CI)	MAPE (95%CI)
0.0 to 1.0	0.589 [0.514, 0.653]	0.430 [0.407, 0.450]
0.5 to 1.5	0.660 [0.550, 0.742]	0.453 [0.431, 0.474]
1.0 to 2.0	0.683 [0.604, 0.753]	0.416 [0.396, 0.445]
1.5 to 2.5	0.691 [0.621, 0.766]	0.271 [0.246, 0.297]
2.0 to 3.0	0.689 [0.616, 0.785]	0.319 [0.282, 0.344]

Table 11: **External validation of predictions of reclassification in Michigan Urological Surgery Improvement Collaborative Active Surveillance cohort.** The area under the receiver operating characteristic curve or AUC (measure of discrimination) and mean absolute prediction error or MAPE (measure of calibration) are calculated over the follow-up period at a gap of 6 months. In addition bootstrapped 95% confidence intervals (CI) are also presented.

Follow-up period (years)	AUC (95% CI)	MAPE (95%CI)
0.0 to 1.0	0.639 [0.607, 0.672]	0.461 [0.450, 0.469]
0.5 to 1.5	0.617 [0.588, 0.652]	0.446 [0.441, 0.453]
1.0 to 2.0	0.599 [0.553, 0.632]	0.331 [0.317, 0.348]

156 Appendix C. Personalized Biopsies Based on Risk of Reclassifica- 157 tion

158 Consider some real patients from the PRIAS database shown in Figure 9
159 to Figure 11. We intend to develop personalized schedule of biopsies for these
160 patients. Using the joint model fitted to the PRIAS dataset, we first obtain
161 their cumulative risk of reclassification over the entire follow-up period (see
162 Equation 4, given their accumulated clinical data. Assume a new patient j
163 whose latest biopsy was conducted at time t and who has visited the clinic
164 at the current time s . We suggest a biopsy at his current visit time s if
165 his cumulative risk of reclassification at s given by $R_j(s | t)$ (Appendix
166 B) is above a certain threshold (e.g., 10% risk). As an example, let us
167 assume that using this rule we decide to schedule a biopsy at time s . Since
168 this patient may be removed from AS upon detection of reclassification, the
169 schedule of remaining future biopsies can only be made under the assumption
170 that reclassification could not be observed at s . Under this assumption we
171 update the patient's cumulative risk of reclassification at next visit time
172 $s + 1$ to be $R_j(s + 1 | s)$. Now, if $R_j(s + 1 | s) < 10\%$, then we will
173 not schedule a biopsy at $s + 1$. Instead, we will decide for a biopsy at a
174 subsequent time $s + 2$ using the cumulative risk $R_j(s + 2 | s)$. If however,
175 at time $s + 1$ the cumulative risk of reclassification $R_j(s + 1 | s) \geq 10\%$
176 then we would have decided for a biopsy at $s + 1$. Consequently, the biopsy
177 decision at time $s + 2$ would have been made using the updated cumulative
178 risk $R_j(s + 2 | s + 1)$ and not $R_j(s + 2 | s)$. We repeat this process for a
179 fixed horizon in each cohort (PRIAS and five external GAP3 cohorts). This
180 horizon is the maximum time point t_h , such that there are at least 10 patients
181 who experience reclassification after t_h (Table 12). This horizon is six years
182 in PRIAS. While scheduling these biopsies we always maintain a minimum
183 gap of one year, as recommended in PRIAS. Personalized schedules can also
184 be made with any other risk threshold such as 5% or 15%.

To assist patients in making an informed choice for a schedule, be it per-
sonalized or fixed, we provide them patient-specific consequences of following
each schedule. To this end, we first calculate the probability of occurrence
of reclassification between successive biopsies of each schedule. Using these
probabilities we then obtain the expected delay in detection of reclassifica-
tion for following that schedule. Thus, patients have a method to compare
across various schedules in terms of the personalized burden (time and total
biopsies), and personalized benefit (less delay in detection of reclassification

Table 12: **Maximum follow-up period up to which we can reliably make personalized schedules.** In each cohort, this time point is chosen such that there are at least 10 patients who experience reclassification after this time point. Full names of Cohorts are *PRIAS*: Prostate Cancer International Active Surveillance, *Toronto*: University of Toronto Active Surveillance, *Hopkins*: Johns Hopkins Active Surveillance, *MSKCC*: Memorial Sloan Kettering Cancer Center Active Surveillance, *KCL*: King's College London Active Surveillance, *MUSIC*: Michigan Urological Surgery Improvement Collaborative Active Surveillance.

Cohort	Maximum Personalized Schedule Time (years)
PRIAS	6
KCL	3
MUSIC	2
Toronto	8
MSKCC	6
Hopkins	7

is beneficial). Suppose once again that for patient j , the time of latest negative biopsy is t_0 , and current visit time is $s > t_0$. Then equation for the expected delay $D_j(\mathcal{S} \mid t, s)$ in detection of reclassification using schedule of biopsies $\mathcal{S} = \{t_1, \dots, t_h\}$, where $t_1 \geq s$, and t_h is the horizon time up to which we want to schedule biopsies, is given by:

$$D_j(\mathcal{S} \mid t, s) = \sum_{v=1}^h R_j(t_v \mid t_{v-1}, s) \times \left\{ t_v - t_{v-1} - \int_{t_{v-1}}^{t_v} S_j(u \mid t_v, t_{v-1}, s) du \right\},$$

$$S_j(u \mid t_v, t_{v-1}, s) = \Pr\{T_j^* > u \mid t_v \geq T_j^* > t_{v-1}, \mathcal{Y}_j(s), \mathcal{D}_n\}, \quad t_v \geq u > t_{v-1}, \quad (6)$$

185 and $R_j(t_v \mid t_{v-1}, s)$ is as defined in Equation (4). The personalized and fixed
186 schedules, and their consequences for a few real patients from the PRIAS
187 dataset are shown in Figure 9 to Figure 11. A compulsory biopsy was done
188 at horizon t_h of follow-up in all schedules for meaningful comparison of their
189 expected delays in detection of reclassification.

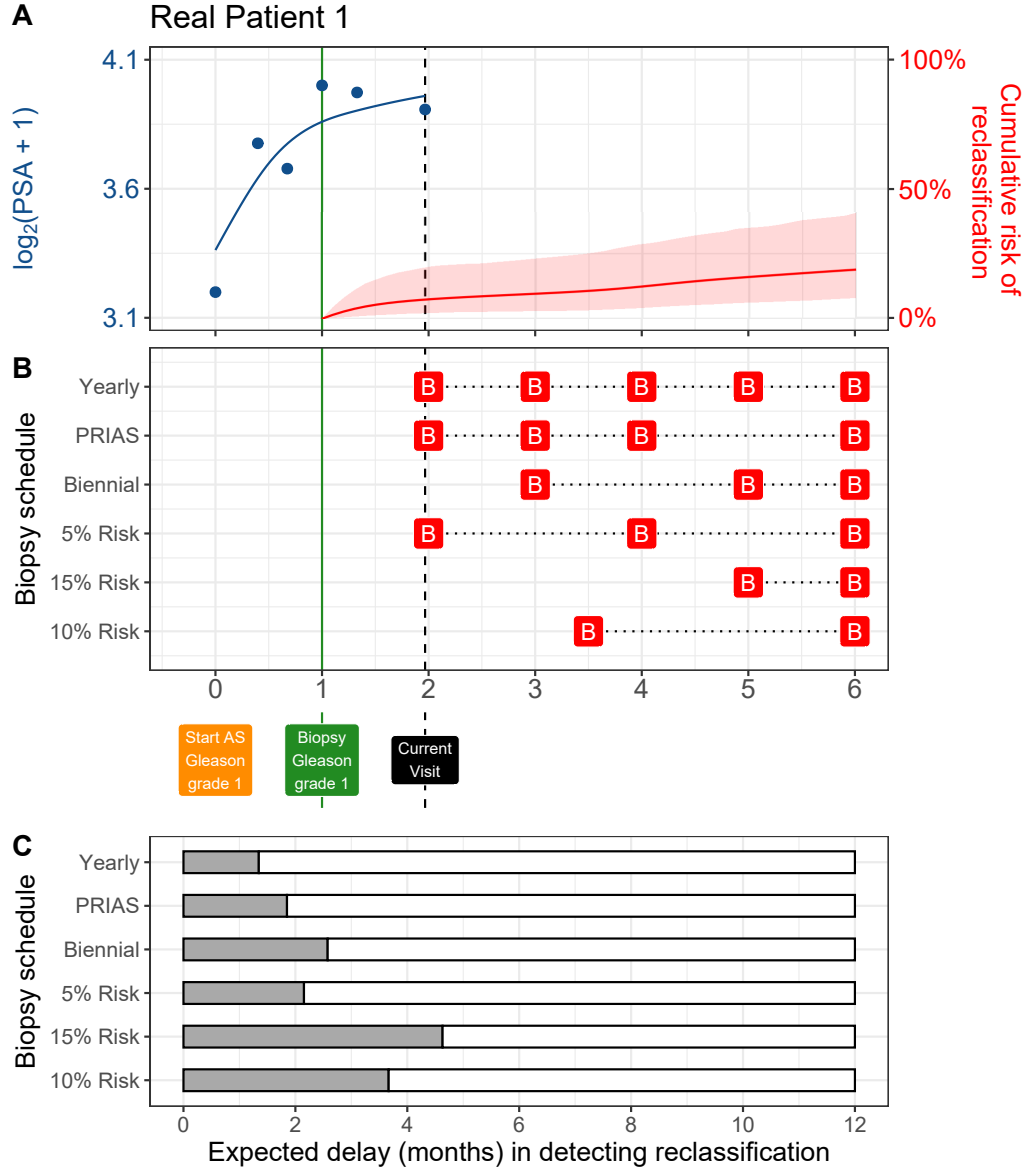


Figure 9: **Personalized and fixed schedules of biopsies for patient 1.** **Panel A:** shows the observed and fitted $\log_2(\text{PSA} + 1)$ measurements (Equation 1), and the dynamic cumulative risk of reclassification (see Appendix B) over follow-up period. **Panel B** shows the personalized and fixed schedules of biopsies with a 'B' indicating times of biopsies. **Panel C** various schedules are compared in terms of the expected delay in detection of reclassification if they are followed.

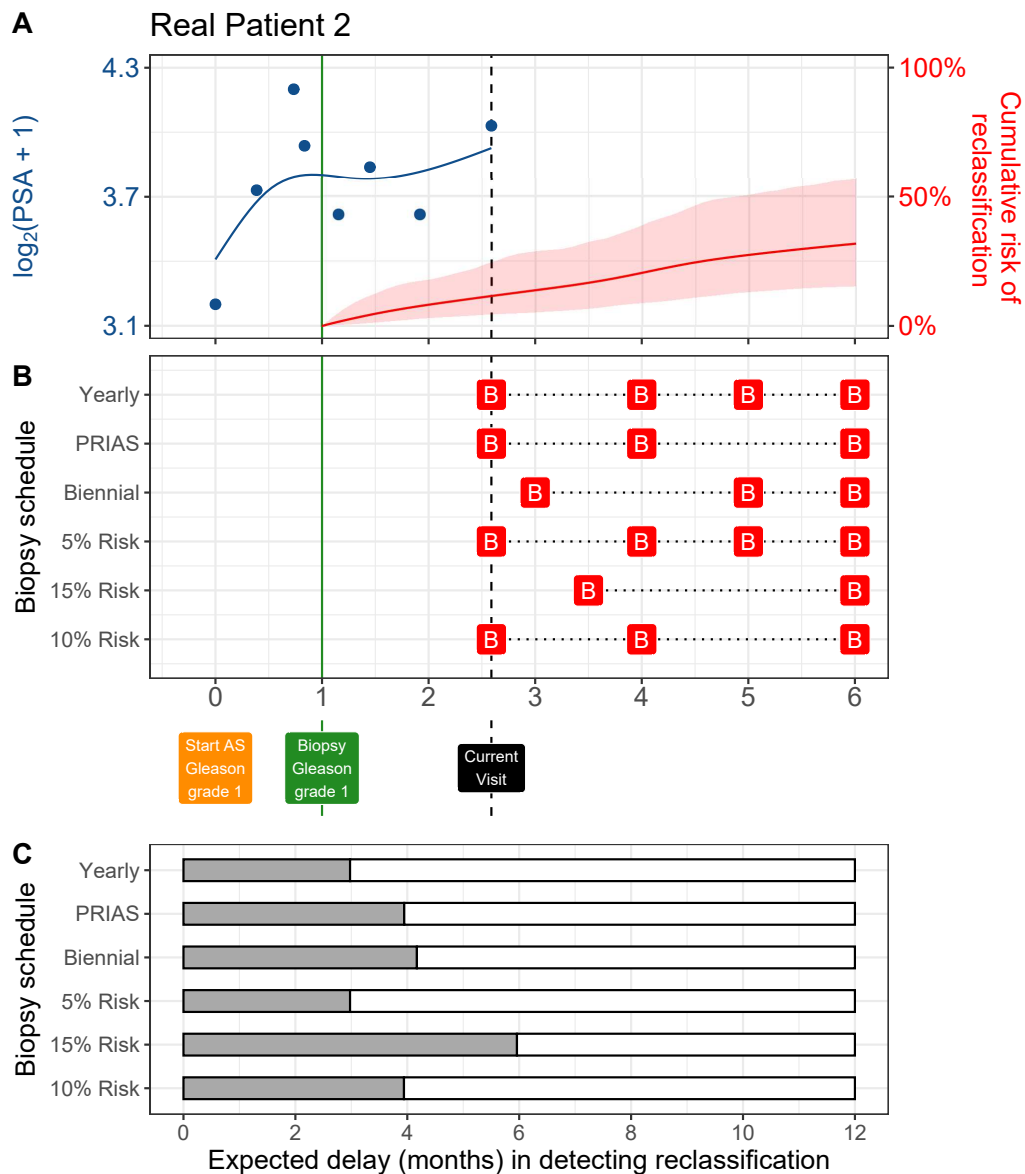


Figure 10: **Personalized and fixed schedules of biopsies for patient 2.** **Panel A:** shows the observed and fitted $\log_2(\text{PSA} + 1)$ measurements (Equation 1), and the dynamic cumulative risk of reclassification (see Appendix B) over follow-up period. **Panel B** shows the personalized and fixed schedules of biopsies with a 'B' indicating times of biopsies. **Panel C** compares various schedules in terms of the expected delay in detection of reclassification if they are followed.

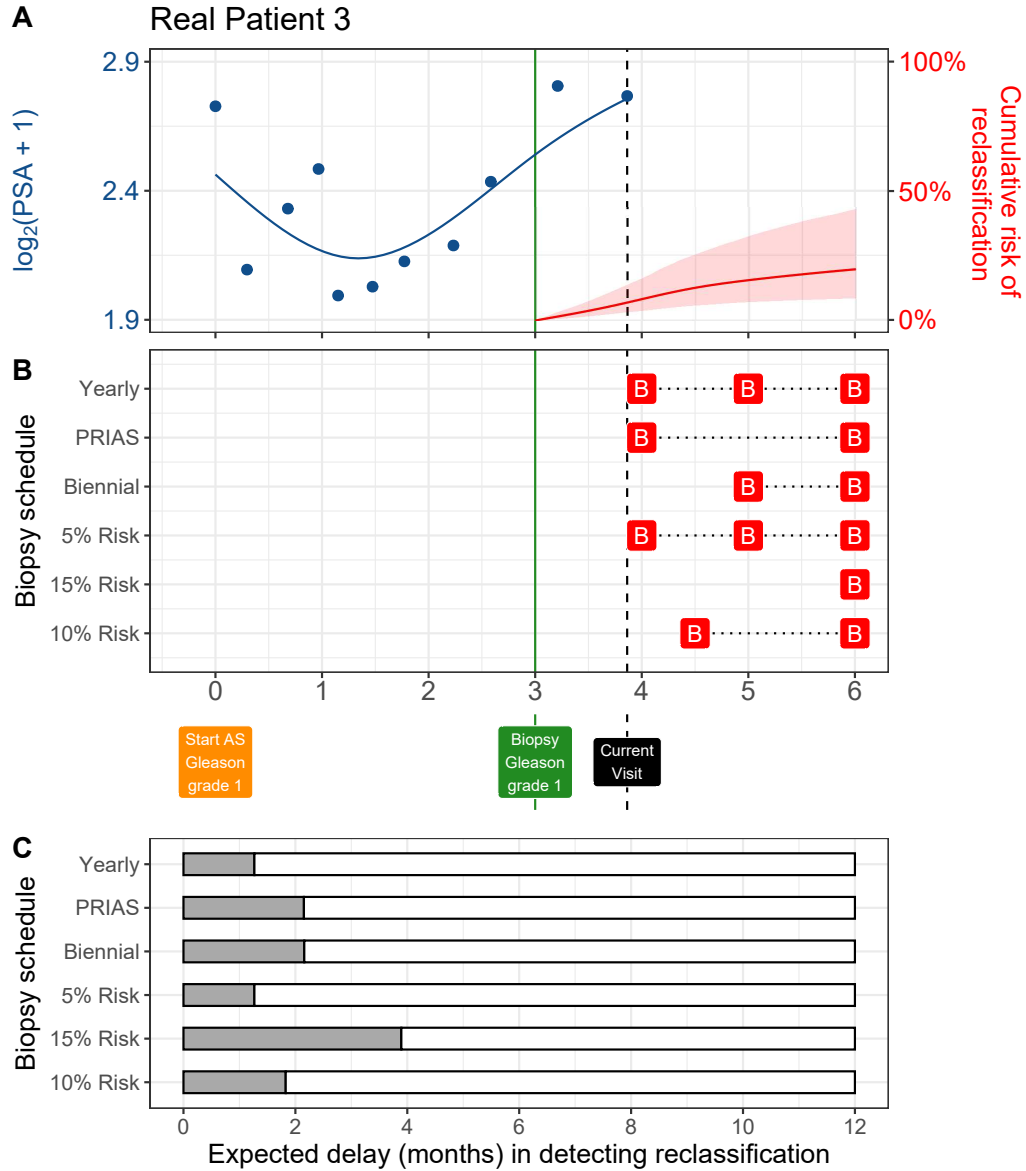


Figure 11: **Personalized and fixed schedules of biopsies for patient 3.** **Panel A:** shows the observed and fitted $\log_2(\text{PSA} + 1)$ measurements (Equation 1), and the dynamic cumulative risk of reclassification (see Appendix B) over follow-up period. **Panel B** shows the personalized and fixed schedules of biopsies with a ‘B’ indicating times of biopsies. **Panel C** compares various schedules in terms of the expected delay in detection of reclassification if they are followed.

Appendix D. Web Application for Practical Use of Personalized Schedule of Biopsies

We implemented our methodology in a web-application to assist patients and doctors in better decision making. It works on desktop as well as mobile devices. The cohorts that are currently supported in this web-application are PRIAS and the largest five cohorts from the GAP3 database [7]. These are the University of Toronto AS (Toronto), Johns Hopkins AS (Hopkins), Memorial Sloan Kettering Cancer Center AS (MSKCC), King's College London AS (KCL), and Michigan Urological Surgery Improvement Collaborative AS (MUSIC). The web-application is hosted at https://emcbiostatistics.shinyapps.io/prias_biopsy_recommender/.

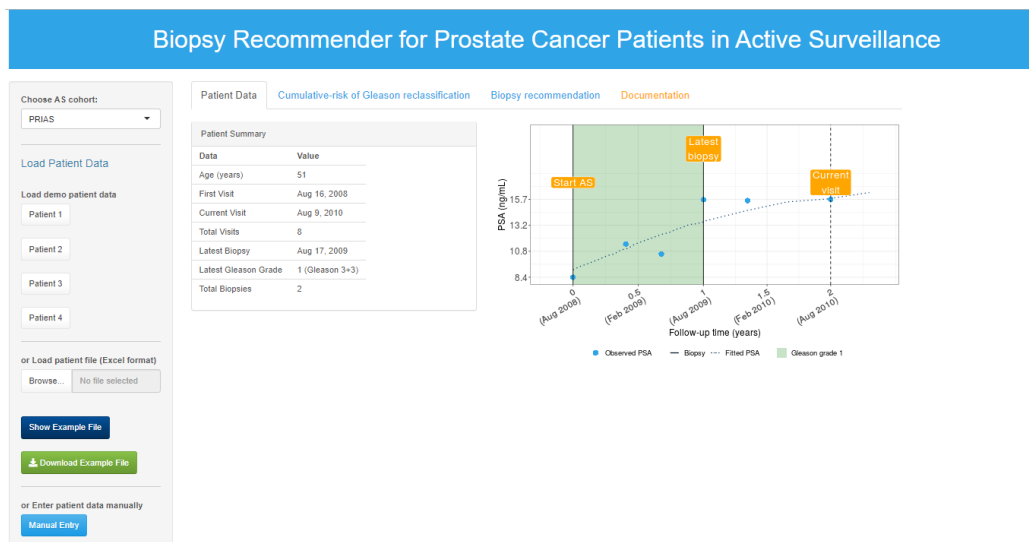


Figure 12: Landing page of the web-application. Panel on the left allows users to load patient data and panel on the right provides information. Patient data can be entered manually, or via Excel files. In addition, demo patient data is already uploaded to assist users in understanding the web-application.

201 Appendix E. Source Code

202 The R code for fitting the joint model to the PRIAS dataset, is at https://github.com/anirudhtomer/prias/tree/master/src/clinical_gap3. We
 203 refer to this location as ‘R_HOME’ in the rest of this document.
 204

205 Appendix E.1. Fitting the Joint Model to the PRIAS dataset

206 **Accessing the dataset:** The PRIAS dataset is not openly accessible.
 207 However, access to the database can be requested via the contact links at
 208 <https://www.prias-project.org>.
 209

210 **Formatting the dataset:** This dataset however is in the so-called wide
 211 format and also requires removal of incorrect entries. This can be done via
 212 the R script `R_HOME/dataset_cleaning.R`. This will lead to two R objects,
 213 namely ‘`prias_final.id`’ and ‘`prias_long_final`’. The ‘`prias_final.id`’ object con-
 214 tains information about time of reclassification for PRIAS patients. The
 215 ‘`prias_long_final`’ object contains longitudinal PSA measurements, the time
 216 of biopsies and results of biopsies.
 217

218 **Fitting the joint model:** We use a joint model for time to event and
 219 longitudinal data to model the evolution of PSA measurements over time,
 220 and to simultaneously model their association with the risk of reclassification.
 221 The R package we use for this purpose is called **JMbayes** ([https://cran.r-](https://cran.r-project.org/web/packages/JMbayes/JMbayes.pdf)
 222 [project.org/web/packages/JMbayes/JMbayes.pdf](https://cran.r-project.org/web/packages/JMbayes/JMbayes.pdf)). The API we use, how-
 223 ever, are currently not hosted on CRAN, and can be found here: [https:](https://github.com/anirudhtomer/JMbayes)
 224 [//github.com/anirudhtomer/JMbayes](https://github.com/anirudhtomer/JMbayes). The joint model can be fitted via
 225 the script `R_HOME/analysis.R`. It takes roughly 6 hours to run on an Intel
 226 core-i5 machine with 4 cores, and 8GB of RAM.

227 The graphs presented in the main manuscript, and the supplementary
 228 material can be generated by the scripts in `R_HOME/plots/`.

229 Appendix E.2. Validation of Predictions of Reclassification

230 Validations can be done using the scripts `R_HOME/validation/auc_brier/`
 231 `auc_calculator.R`, and `R_HOME/validation/auc_brier/gof_calculator.`
 232 `R`. For external validation access to GAP3 database is required.

233 *Appendix E.3. Creating Personalized Schedules of Biopsies*

234 Once a joint model is fitted to the PRIAS dataset, personalized schedules
235 of biopsies based on risk of reclassification for new patients can be devel-
236 oped using the script `R_HOME/scheduleCreator.R`. This script also provides
237 fixed biopsy schedules for the patients. In addition with each schedule, the
238 expected delay in detection of reclassification is also provided.

239 *Appendix E.4. Source Code for Web Application*

240 Source for the shiny web application which provides biopsy schedules for
241 patients can be found at `R_HOME/shinyapp`

242 **Appendix F. Appendix A. Members of The Movember Founda-**
 243 **tions Global Action Plan Prostate Cancer Active Surveil-**
 244 **lance (GAP3) consortium**

245 *Principle Investigators:* Bruce Trock (Johns Hopkins University, The
 246 James Buchanan Brady Urological Institute, Baltimore, USA), Behfar Ehdaie
 247 (Memorial Sloan Kettering Cancer Center, New York, USA), Peter Car-
 248 roll (University of California San Francisco, San Francisco, USA), Christo-
 249 pher Filson (Emory University School of Medicine, Winship Cancer Insti-
 250 tute, Atlanta, USA), Jeri Kim / Christopher Logothetis (MD Anderson
 251 Cancer Centre, Houston, USA), Todd Morgan (University of Michigan and
 252 Michigan Urological Surgery Improvement Collaborative (MUSIC), Michi-
 253 gan, USA), Laurence Klotz (University of Toronto, Sunnybrook Health Sci-
 254 ences Centre, Toronto, Ontario, Canada), Tom Pickles (University of British
 255 Columbia, BC Cancer Agency, Vancouver, Canada), Eric Hyndman (Uni-
 256 versity of Calgary, Southern Alberta Institute of Urology, Calgary, Canada),
 257 Caroline Moore (University College London & University College London
 258 Hospital Trust, London, UK), Vincent Gnanapragasam (University of Cam-
 259 bridge & Cambridge University Hospitals NHS Foundation Trust, Cam-
 260 bridge, UK), Mieke Van Hemelrijck (King's College London, London, UK
 261 & Guys and St Thomas NHS Foundation Trust, London, UK), Prokar Das-
 262 gupta (Guys and St Thomas NHS Foundation Trust, London, UK), Chris
 263 Bangma (Erasmus Medical Center, Rotterdam, The Netherlands/ represen-
 264 tative of Prostate cancer Research International Active Surveillance (PRIAS)
 265 consortium), Monique Roobol (Erasmus Medical Center, Rotterdam, The
 266 Netherlands/ representative of Prostate cancer Research International Active
 267 Surveillance (PRIAS) consortium), Arnauld Villers (Lille University Hospi-
 268 tal Center, Lille, France), Antti Rannikko (Helsinki University and Helsinki
 269 University Hospital, Helsinki, Finland), Riccardo Valdagni (Department of
 270 Oncology and Hemato-oncology, Universit degli Studi di Milano, Radia-
 271 tion Oncology 1 and Prostate Cancer Program, Fondazione IRCCS Istituto
 272 Nazionale dei Tumori, Milan, Italy), Antoinette Perry (University College
 273 Dublin, Dublin, Ireland), Jonas Hugosson (Sahlgrenska University Hospital,
 274 Gteborg, Sweden), Jose Rubio-Briones (Instituto Valenciano de Oncologa,
 275 Valencia, Spain), Anders Bjartell (Skne University Hospital, Malm, Swe-
 276 den), Lukas Hefermehl (Kantonsspital Baden, Baden, Switzerland), Lee Lui
 277 Shiong (Singapore General Hospital, Singapore, Singapore), Mark Fryden-
 278 berg (Monash Health; Monash University, Melbourne, Australia), Yoshiyuki

279 Kakehi / Mikio Sugimoto (Kagawa University Faculty of Medicine, Kagawa,
280 Japan), Byung Ha Chung (Gangnam Severance Hospital, Yonsei University
281 Health System, Seoul, Republic of Korea)

282 *Pathologist:* Theo van der Kwast (Princess Margaret Cancer Centre,
283 Toronto, Canada). Technology Research Partners: Henk Obbink (Royal
284 Philips, Eindhoven, the Netherlands), Wim van der Linden (Royal Philips,
285 Eindhoven, the Netherlands), Tim Hulsén (Royal Philips, Eindhoven, the
286 Netherlands), Cees de Jonge (Royal Philips, Eindhoven, the Netherlands).

287 *Advisory Regional statisticians:* Mike Kattan (Cleveland Clinic, Cleve-
288 land, Ohio, USA), Ji Xinge (Cleveland Clinic, Cleveland, Ohio, USA), Ken-
289 neth Muir (University of Manchester, Manchester, UK), Artitaya Lophatananon
290 (University of Manchester, Manchester, UK), Michael Fahey (Epworth Health-
291 Care, Melbourne, Australia), Ewout Steyerberg (Erasmus Medical Center,
292 Rotterdam, The Netherlands), Daan Nieboer (Erasmus Medical Center, Rot-
293 terdam, The Netherlands); Liying Zhang (University of Toronto, Sunnybrook
294 Health Sciences Centre, Toronto, Ontario, Canada)

295 *Executive Regional statisticians:* Ewout Steyerberg (Erasmus Medical
296 Center, Rotterdam, The Netherlands), Daan Nieboer (Erasmus Medical Cen-
297 ter, Rotterdam, The Netherlands); Kerri Beckmann (King's College London,
298 London, UK & Guys and St Thomas NHS Foundation Trust, London, UK),
299 Brian Denton (University of Michigan, Michigan, USA), Andrew Hayen (Uni-
300 versity of Technology Sydney, Australia), Paul Boutros (Ontario Institute of
301 Cancer Research, Toronto, Ontario, Canada).

302 *Clinical Research Partners IT Experts:* Wei Guo (Johns Hopkins Uni-
303 versity, The James Buchanan Brady Urological Institute, Baltimore, USA),
304 Nicole Benfante (Memorial Sloan Kettering Cancer Center, New York, USA),
305 Janet Cowan (University of California San Francisco, San Francisco, USA),
306 Dattatraya Patil (Emory University School of Medicine, Winship Cancer In-
307 stitute, Atlanta, USA), Emily Tolosa (MD Anderson Cancer Centre, Hous-
308 ton, Texas, USA), Tae-Kyung Kim (University of Michigan and Michigan
309 Urological Surgery Improvement Collaborative, Ann Arbor, Michigan, USA),
310 Alexandre Mamedov (University of Toronto, Sunnybrook Health Sciences
311 Centre, Toronto, Ontario, Canada), Vincent LaPointe (University of British
312 Columbia, BC Cancer Agency, Vancouver, Canada), Trafford Crump (Uni-
313 versity of Calgary, Southern Alberta Institute of Urology, Calgary, Canada),
314 Vasilis Stavrinos (University College London & University College Lon-
315 don Hospital Trust, London, UK), Jenna Kimberly-Duffell (University of
316 Cambridge & Cambridge University Hospitals NHS Foundation Trust, Cam-

bridge, UK), Aida Santaolalla (King's College London, London, UK & Guys
and St Thomas NHS Foundation Trust, London, UK), Daan Nieboer (Eras-
mus Medical Center, Rotterdam, The Netherlands), Jonathan Olivier (Lille
University Hospital Center, Lille, France), Tiziana Rancati (Fondazione IR-
CCS Istituto Nazionale dei Tumori di Milano, Milan, Italy), Heln Ahlgren
(Sahlgrenska University Hospital, Gteborg, Sweden), Juanma Mascars (Insti-
tuto Valenciano de Oncologa, Valencia, Spain), Annica Lfgren (Skne Univer-
sity Hospital, Malm, Sweden), Kurt Lehmann (Kantonsspital Baden, Baden,
Switzerland), Catherine Han Lin (Monash University and Epworth Health-
Care, Melbourne, Australia), Hiromi Hiram (Kagawa University, Kagawa,
Japan), Kwang Suk Lee (Yonsei University College of Medicine, Gangnam
Severance Hospital, Seoul, Korea).

Research Advisory Committee: Guido Jenster (Erasmus MC, Rotterdam,
the Netherlands), Anssi Auvinen (University of Tampere, Tampere, Finland),
Anders Bjartell (Skne University Hospital, Malm, Sweden), Masoom Haider
(University of Toronto, Toronto, Canada), Kees van Bochove (The Hyve
B.V. Utrecht, Utrecht, the Netherlands), Ballentine Carter (Johns Hopkins
University, Baltimore, USA until 2018).

Management team: Sam Gledhill (Movember Foundation, Melbourne,
Australia), Mark Buzza / Michelle Kouspou (Movember Foundation, Mel-
bourne, Australia), Chris Bangma (Erasmus Medical Center, Rotterdam,
The Netherlands), Monique Roobol (Erasmus Medical Center, Rotterdam,
The Netherlands), Sophie Bruinsma / Jozien Helleman (Erasmus Medical
Center, Rotterdam, The Netherlands).

References

1. Epstein JI, Egevad L, Amin MB, Delahunt B, Srigley JR, Humphrey PA.
The 2014 international society of urological pathology (isup) consensus
conference on gleason grading of prostatic carcinoma. *The American
journal of surgical pathology* 2016;40(2):244–52.
2. Pearson JD, Morrell CH, Landis PK, Carter HB, Brant LJ. Mixed-
effects regression models for studying the natural history of prostate
disease. *Statistics in Medicine* 1994;13(5-7):587–601.
3. Lin H, McCulloch CE, Turnbull BW, Slate EH, Clark LC. A latent
class mixed model for analysing biomarker trajectories with irregularly
scheduled observations. *Statistics in Medicine* 2000;19(10):1303–18.

- 352 4. De Boor C. A practical guide to splines; vol. 27. Springer-Verlag New
353 York; 1978.
- 354 5. Eilers PH, Marx BD. Flexible smoothing with B-splines and penalties.
355 *Statistical Science* 1996;11(2):89–121.
- 356 6. Turnbull BW. The empirical distribution function with arbitrarily
357 grouped, censored and truncated data. *Journal of the Royal Statisti-*
358 *cal Society Series B (Methodological)* 1976;38(3):290–5.
- 359 7. Bruinsma SM, Zhang L, Roobol MJ, Bangma CH, Steyerberg EW,
360 Nieboer D, Van Hemelrijck M, consortium MFGAPPCASG, Troock B,
361 Ehdaie B, et al. The mover foundation’s gap3 cohort: a profile of
362 the largest global prostate cancer active surveillance database to date.
363 *BJU international* 2018;121(5):737–44.
- 364 8. Rizopoulos D. The R package JMBayes for fitting joint models for lon-
365 gitudinal and time-to-event data using MCMC. *Journal of Statistical*
366 *Software* 2016;72(7):1–46.
- 367 9. Rizopoulos D, Molenberghs G, Lesaffre EM. Dynamic predictions with
368 time-dependent covariates in survival analysis using joint modeling and
369 landmarking. *Biometrical Journal* 2017;59(6):1261–76.
- 370 10. Steyerberg EW, Vickers AJ, Cook NR, Gerds T, Gonen M, Obuchowski
371 N, Pencina MJ, Kattan MW. Assessing the performance of prediction
372 models: a framework for some traditional and novel measures. *Epidemi-*
373 *ology (Cambridge, Mass)* 2010;21(1):128.
- 374 11. Bokhorst LP, Alberts AR, Rannikko A, Valdagni R, Pickles T, Kakehi Y,
375 Bangma CH, Roobol MJ, PRIAS study group . Compliance rates with
376 the Prostate Cancer Research International Active Surveillance (PRIAS)
377 protocol and disease reclassification in noncompliers. *European Urology*
378 2015;68(5):814–21.